The Journal of Immunology

# Dual Functions of Bruton's Tyrosine Kinase and Tec Kinase during Fc γ Receptor-Induced Signaling and Phagocytosis

Jenny Jongstra-Bilen, Adrianet Puig Cano, Manvi Hasija, Haiyan Xiao, C. I. Edvard Smith and Myron I. Cybulsky

*J Immunol* 2008; 181:288-298; ;
doi: 10.4049/jimmunol.181.1.288
http://www.jimmunol.org/content/181/1/288





*The Journal of Immunology* is published twice each month by
The American Association of Immunologists, Inc.,
1451 Rockville Pike, Suite 650, Rockville, MD 20852

Print ISSN: 0022-1767 Online ISSN: 1550-6606.

# Dual Functions of Bruton's Tyrosine Kinase and Tec Kinase during Fcγ Receptor-Induced Signaling and Phagocytosis[1]

**Jenny Jongstra-Bilen,[2]*†‡ Adrianet Puig Cano,* Manvi Hasija,* Haiyan Xiao,* C. I. Edvard Smith,[§] and Myron I. Cybulsky*‡**

**Tec family nonreceptor tyrosine kinases are expressed by hematopoietic cells, activate phospholipase C (PLC)γ, and regulate cytoskeletal rearrangement, yet their role in FcγR-induced signaling and phagocytosis remains unknown. We demonstrate in this study that Bruton's tyrosine kinase (Btk) and Tec, the only Tec kinases expressed by RAW 264.7 cells, are activated throughout phagocytosis. Activated Btk and Tec kinase accumulate at an early stage at the base of phagocytic cups and inhibition of their activity by the specific inhibitor LFM-A13 or expression by small interfering RNA significantly inhibited FcγR-induced phagocytosis. Similarly, a significant role for these kinases in phagocytosis was found in primary macrophages. FcγR-induced activation of Mac-1, which is required for optimal phagocytosis, was markedly inhibited and our findings suggest that the roles of kinases Btk and Tec in Mac-1 activation account for their functions in the early stages of phagocytosis. Initial activation of PLCγ2, the predominant PLC isoform in RAW 264.7 cells, is dependent on Syk. In contrast, a late and prolonged activation of PLCγ2 was dependent on Btk and Tec. We found accumulation of diacylglycerol (DAG), a PLCγ product, in phagosome membranes, and activated Btk, but not Tec, colocalized with phagosomal DAG. Inhibition of Tec family kinase activity increased the level of DAG in phagosomes, suggesting a negative regulatory role for Btk. Tec, in contrast, clustered at sites near phagosome formation. In summary, we elucidated that Tec family kinases participate in at least two stages of FcγR-mediated phagocytosis: activation of Mac-1 during ingestion, and after phagosome formation, during which Btk and Tec potentially have distinct roles.** ***The Journal of Immunology,*** **2008, 181: 288–298.**

Phagocytosis is an essential process that involves engulfment and clearing of microbial pathogens and is conducted most efficiently by monocytes/macrophages or neutrophils (1). The ingestion of IgG-opsonized targets is initiated by the engagement and clustering of FcγRs, which induce receptor tyrosine phosphorylation by Src family kinases and recruitment of the tyrosine kinase Syk to the phosphorylated FcγR chain (2, 3). The subsequent activation of multiple downstream signaling pathways results in the formation of a phagocytic cup beneath the adherent particle and the extension of pseudopods around it. Cup formation is mediated by local actin polymerization, cytoskeletal rearrangement, and membrane remodeling. The subsequent fusion of the pseudopods results in the closure of the cup to form a vacuole called a phagosome (4, 5). Phagosomes are internalized and undergo dramatic changes in the membrane and contents due to a progressive maturation process that ultimately results in the formation of phagolysosome, at which the degradation and clearing of pathogens occurs (6, 7).

One of the early molecular switches that control these complex events is Syk activation (8, 9). However, the pathways controlled by Syk have not been fully characterized. The analysis of $Syk^{-/-}$ macrophages revealed that Syk activity is important for phagosome closure and ingestion of IgG-opsonized particles downstream of particle binding and actin polymerization (10, 11). Local F-actin polymerization is in part dependent on type Iα phosphatidylinositol-4-phosphate 5-kinase, the enzyme responsible for phosphatidylinositol 4,5-bisphosphate ($PIP_2$)[3] generation (12–14). $PIP_2$ accumulates at particle binding sites and extending pseudopods within minutes of FcγR engagement. Botelho et al. (15) showed that this accumulation is transient and is lost rapidly before the closure of the phagocytic cup. There is evidence that phospholipase C (PLC)γ activity accounts at least in part for the disappearance of $PIP_2$ by its hydrolysis to form diacylglycerol (DAG) and inositol 3,4,5-triphosphate. PLCγ is recruited to the phagocytic cup and the loss of $PIP_2$ was accompanied by the accumulation of DAG at the base of the phagocytic cup (15). DAG can be generated through the activities of phospholipase D or PLC, and there is support for the involvement of both enzymes in phagocytosis (15–17). Recently, PLCγ-derived DAG was shown to be important for the activation of protein kinase C (PKC)ε, which accumulates at phagocytic cups and plays a critical role in FcγR-mediated phagocytosis (18, 19).

The Tec family of cytoplasmic tyrosine kinases includes Bruton's tyrosine kinase (Btk), Tec, Itk (Emt), Rlk (Txk), and Bmx

*Toronto General Research Institute, University Health Network, and †Department of Immunology and ‡Department of Laboratory Medicine and Pathobiology, University of Toronto, Toronto, Ontario Canada; and §Department of Laboratory Medicine, Karolinska Institutet, Huddinge, Sweden

Received for publication July 16, 2007. Accepted for publication April 24, 2008.

The costs of publication of this article were defrayed in part by the payment of page charges. This article must therefore be hereby marked *advertisement* in accordance with 18 U.S.C. Section 1734 solely to indicate this fact.

[1] This work was supported by Grant RGPIN 194609-3 from the Natural Sciences and Engineering Research Council of Canada (to J.J.-B.) and Grant MOP-14151 from the Canadian Institutes of Health Research (to M.I.C.). C.I.E.S. is supported by the Swedish Cancer Foundation. M.I.C. is a career investigator of the Heart and Stroke Foundation of Ontario.

[2] Address correspondence and reprint requests to Dr. Jenny Jongstra-Bilen, Max Bell Research Centre, Room 1R-408, Toronto General Research Hospital, University Health Network, 200 Elizabeth Street, Toronto, Ontario M5G 2C4, Canada. E-mail address: jbilen@uhnres.utoronto.ca

[3] Abbreviations used in this paper: $PIP_2$, phosphatidylinositol 4,5-bisphosphate; aggIgG, aggregated IgG; Btk, Bruton's tyrosine kinase; DAG, diacylglycerol; DIC, differential interference contrast; PKC, protein kinase C; XLA, X-linked agammaglobulinemia; siRNA, small interfering RNA; PLC, phospholipase C; $PIP_3$, phosphatidylinositol 3,4,5-trisphosphate.

(Etk). These kinases are expressed predominantly in hematopoietic cells and are involved in a variety of cellular functions including $Ca^{2+}$ influx, cytoskeletal remodeling, gene expression, survival, apoptosis, proliferation, or differentiation (20, 21). The multimodular structure of these kinases and the multitude of binding partners certainly contribute to the diverse functions of these kinases. Among myeloid cells, macrophages and neutrophils express Btk, Tec, and Bmx (22). Several functions of neutrophils such as chemotaxis, adhesion, superoxide production, or degranulation stimulated by fMLP or FcγRIIIb were shown to be dependent on Tec family kinase activity (23, 24). Recently, Amoras et al. (25) reported reduced levels of chemotaxis and FcγR- or complement receptor-mediated phagocytosis in blood monocytes from X-linked agammaglobulinemia (XLA) patients. XLA is a B cell deficiency caused by mutations in the *Btk* gene, which disrupt the functioning of this protein (21, 26). The mechanisms of Btk involvement and the requirement for other Tec family kinases in FcγR-induced phagocytosis have not been investigated. However, Btk and Tec activation through CD32 cross-linking in platelets and Tec activation through FcγRIIIB (CD16b) in human neutrophils suggest that these enzymes are functioning downstream from FcγR signaling (24, 27). PLCγ2 was shown to be a target for Tec family kinases through FcγRIIIB signaling in neutrophils (24). During Ag receptor signaling in lymphocytes, Tec family kinases participate in PLCγ phosphorylation and activation by forming signaling complexes with the adaptor proteins BLNK/SLP-65 in B cells and with LAT and SLP-76 in T cells (28, 29). Murine bone marrow macrophages express uniquely both SLP-76 and BLNK, which are coupled to PLCγ2 activation via FcγRI and FcγRIII (30). Thus, it is possible that FcγR-induced Tec kinases take part in the activation of PLCγ2 during phagocytosis by forming complexes that include these adaptor proteins. PLCγ2 clustered at phagocytic cups may be part of such complexes. However, PLCγ2 involvement in FcγR-mediated phagocytosis has recently been questioned (19). This is primarily because phagocytosis through FcγR was not significantly affected by PLCγ2 deficiency in macrophages from PLCγ2$^{-/-}$ mice (19, 31).

Previously we showed that FcγR-induced Mac-1 activation in RAW 264.7 mouse macrophages was dependent on the activation of PLCγ and was required for optimal phagocytosis (32). Currently, we elucidate the involvement of Tec family kinases (Btk and Tec) in FcγR-mediated phagocytosis and Mac-1 activation in RAW 264.7 cells and primary macrophages. We focused on PLCγ2 as a downstream target and show a unique pattern of modulation of its activity by Tec family kinases, which occurs beyond its initial activation by Syk and persists during phagosome formation when a burst of DAG production was observed. Our findings support distinct roles for Btk and Tec in this late phase of phagocytosis.

## Materials and Methods

### *Reagents and Abs*

The following reagents were used: LFM-A13 (α-cyano-β-hydroxy-β-methyl-*N*-(2,5-dibromophenyl) propenamide) and LFM-A11 (α-cyano-β-hydroxy-β-methyl-*N*-(3-fluorophenyl) propenamide) (EMD Biosciences); piceatannol (Calbiochem); SRBC (MP Biomedicals); polystyrene (S/DVB) beads (Bangs Laboratories); C5-depleted serum, human IgG, and poly-L-lysine (Sigma-Aldrich); predesigned small interfering RNA (siRNA) for Btk and Tec and scrambled duplex control RNA (Ambion), Alexa Fluor 555-cholera toxin B and Alexa Fluor 488-phalloidin (Molecular Probes); recombinant protein G-agarose and Opti-MEM (Invitrogen); and DMEM and trypsin (Wisent). The PKCδ-C1GFP cDNA construct was a gift from Dr. S. Grinstein (Cell Biology Program, Hospital for Sick Children, Toronto, Ontario, Canada). The following Abs were used against: SRBC (IgG; Pharmaceuticals Inc. and IgM; Accurate Chemical and Scientific); Tec and phosphotyrosine (clone 4G10; Upstate); phospho-Btk (Cell Signaling Technology); Btk (rabbit polyclonal antiserum prepared against the Src homology 3 domain, (33)) (clones N-20, M-20 and N-17 for Btk, Tec (for immunostaining), and PLC-γ2, respectively; Santa Cruz Biotechnology); actin (Sigma-Aldrich); fluorescinated secondary Abs (Jackson ImmunoResearch Laboratories).

### *Mice and the isolation of peritoneal macrophages*

Female or male C57BL/6 mice, 8- to 12-wk-old, were bred and housed at the University Health Network Animal Facility under sterile conditions. All procedures were approved by the University Health Network Animal Care Committee according to the guidelines of the Canadian Council on Animal Care. Elicited peritoneal macrophages were harvested 4 days after injection of 4% thioglycolate (i.p., 0.8 ml) by lavage with ice-cold PBS (5 ml) containing 5% FBS and penicillin/streptomycin. Cells were washed twice in growth medium containing antibiotics before plating for culture.

### *Cell culture and transfections*

RAW 264.7 mouse macrophage cell line (RAW cells) was cultured in DMEM with 10% heat-inactivated FCS (growth medium) and transferred either to 10-cm tissue-culture plates (for stimulation assays) or onto acid-washed poly-L-lysine-coated (1 μg/ml) glass coverslips (for single cell assays) 1 day before the experiments. For peritoneal macrophage cultures, $0.5 \times 10^6$ cells per well were cultured overnight on poly-L-lysine-coated (10 μg/ml) coverslips in 12-well plates. Unbound cells were washed off after three washes in DMEM, before the experiments. For siRNA transfections, cells were transfected on two subsequent days with duplex RNA (scrambled control, Btk, Tec, or Btk plus Tec siRNA) using Lipofectamine 2000 (1/25 dilution in Opti-MEM; Invitrogen) as described by the supplier. Cells were analyzed 24 h after the second transfection. PKCδC1-GFP cDNA transfections were performed by FugeneHD (at a ratio of 6:2 FugeneHD to cDNA; Roche Applied Science) according to the instructions of the supplier.

### *Phagocytosis and binding assays*

RAW 264.7 mouse macrophage cell line (RAW cells) or peritoneal macrophages were grown on poly-L-lysine-coated coverslips overnight. IgG opsonization of RBC and phagocytosis of IgG-opsonized RBC (IgG-RBC) in DMEM for 30 min were performed as described (32). For binding experiments and immunostainings at the cup, cells exposed to IgG-RBC were incubated for 5 min at 4°C and for 15 min at room temperature, and were washed three times with PBS before fixation. For experiments with inhibitors, cells were left untreated or preincubated with 100 μM LFM-A13, 100 μM LFM-A11, or DMSO (carrier) for 1 h in DMEM before the addition of IgG-RBC. Phagocytic and binding indices were determined by bright-field microscopy and were defined as the number of RBC ingested or bound per 100 cells, respectively, (400–500 total cells were evaluated for each sample). Where indicated, IgG-coated beads (3.87 μm) were used (25 μl/well in 12-well plate). Beads (10% suspension in PBS) were opsonized with 1 mg/ml human IgG for 1 h at 37°C. Extracellularly bound beads were stained with Cy5-anti-human IgG (1/250) for 5 min on ice before fixing. Ingested and extracellular beads were visualized by differential interference contrast (DIC) microscopy.

### *Mac-1 activation assays and Mac-1 blocking*

C3bi-opsonized RBC binding was determined as a measure of Mac-1 activation following incubation of RAW 264.7 mouse macrophage cell line (RAW cells) or peritoneal macrophages with or without 250 μg/ml aggregated IgG (aggIgG) for 20 min. Opsonization of RBC with C3bi, aggIgG preparation, and binding of the C3bi-opsonized RBC were performed as described (32). Where specified, cells were preincubated with 100 μM LFM-A13, 100 μM LFM-A11, or DMSO for the last 1 h during the 2 h of preincubation time in DMEM (serum-starvation) before the initiation of the assay. Mac-1 blocking experiments were performed in siRNA transfected RAW cells by preincubation with 5 μg/ml anti-CD11b Abs (M1/70) (34) for 15 min, as described (32).

### *Immunostaining and live imaging*

Cells were fixed with 4% paraformaldehyde and permeabilized with 0.1% Triton X-100 in PBS containing 100 mM glycine before blocking as described (32). Abs (5 μg/ml) against Btk, phospho-Btk, Tec, or CD11b

(M1/70) were added before incubation with the corresponding Cy3 secondary Abs with Alexa Fluor 488-phalloidin and Cy5-anti-rabbit IgG. Immunostained cells were analyzed by Flowview FV-1000; Olympus confocal microscope with 60X (NA1.4) oil objective. For live imaging of phagocytosis in cells transfected with PKCδC1-GFP, cholera toxin B (2 μg/ml) was added to cells before the addition of IgG-RBC to label the plasma membranes and the phagosomes (35). Images were captured using a spinning disk confocal microscope, Zeiss Axiovert 200 equipped with a Hamamatsu Orca AG charge-coupled device camera, Yokogawa spinning disk confocal scan head, and Improvision Volocity software (version 3.7). The laser lines, 491 and 561 nm, with corresponding filters were used. Analyses of pixel density for GFP (phagosomal membrane vs cytosol) or CD11b (cup vs plasma membrane) were determined by the ImageJ software (version 1.32g).

### *Cell stimulation, immunoprecipitation, and Western blot analysis*

RAW 264.7 mouse macrophage cell line (RAW cells) grown on 10-cm dishes were preincubated with 50 μM piceatannol (30 min) and 100 μM LFM-A13 or 100 μM LFM-A11 (1 h) in DMEM, before the addition of 1 ml of IgG-RBC for different times (0–15 min) at 37°C. After a 20 s hypoosmotic shock to lyse the uningested RBC, cells were washed three times in ice-cold PBS containing the phosphatase inhibitors, 1 mM $Na_3VO_4$ (orthovanadate) and 1 mM NaF. Cells were lysed on the plate by adding buffer A (20 mM Tris-HCl (pH 7.6), 150 mM NaCl, 1% Triton X-100, 10 mM EDTA, 1 mM NaF, 2 mM $Na_3VO_4$, 1 mM PMSF, and one complete protease inhibitor cocktail tablet (Roche)) for 15 min on ice. Lysates were microcentrifuged at 12,000 × *g* for 10 min at 4°C. Lysate supernatants were used for the analysis of protein amounts, immunoprecipitation, or Western blot analysis of tyrosine-phosphorylated proteins. For immunoprecipitations, 1 ml of lysate supernatants (1 mg of protein) were incubated with anti-Btk serum (1/300), 4 μg of anti-Tec, or 1.2 μg of anti-PLCγ2 Abs using an end-over-end rotator for 2 h (Btk, Tec) or overnight (PLCγ2) at 4°C and for an additional 1 h with protein G-agarose (40 μl, 1:1 slurry). The beads were recovered by centrifugation, washed three times with cold buffer A and once with TBS (20 mM Tris-HCl, 150 mM NaCl (pH 7.6)), resuspended in 60 μl of Laemmli loading buffer (36), and boiled for 5 min. Beads were separated from the supernatant by centrifugation and 30 μl of supernatants were loaded on 8% SDS-PAGE along with the lysate supernatants (7.5 μg of protein) collected before immunoprecipitation. Proteins were transferred onto nitrocellulose filters (22 V, overnight) and revealed with anti-phosphotyrosine Abs (4G10, 1/4000) and HRP-conjugated anti-mouse secondary Abs (1/20,000) using ECL Plus detection kit (Amersham Biosciences). The blots were then stripped by incubating the membrane for 1 h at 55°C in 62.5 mM Tris-HCl, 100 mM 2-ME, 2% SDS followed by two washes with TBS-0.1% Tween 20. Blots were reprobed for total immunoprecipitated Btk, Tec, or PLCγ2, as indicated. For quantifications of Btk and Tec expression in siRNA experiments by Western blotting, increasing amounts of whole cell lysates (cell pellets resuspended in Laemmli loading buffer) from control samples were loaded along with the corresponding samples from siRNA transfected cells. Western blots were revealed for Btk, Tec, and for actin to compare the loads. Pixel intensity for Btk, Tec, and actin bands was determined by the ImageJ software (version 1.32g). Control and siRNA samples with equivalent actin loads were compared.

### *RNA preparation, reverse transcription, and primer synthesis*

Total RNA was isolated from RAW cells, splenocytes, and peritoneal macrophages using the RNeasy kit (Qiagen) to measure Tec family kinase gene expression. Total RNA samples from siRNA transfectants in 24-well plates were isolated using the PicoPure RNA isolation kit (Arcturus). Reverse transcription into single-stranded cDNA was performed using random primers (Invitrogen) and the Powerscript kit (Clontech Laboratories). The following primers for Tec family kinase genes were designed using the Primer Express software (Applied Biosystems): *Btk*, forward GAGTAACATTCTAGATGT GATGG and reverse CAGTCTGTTAGGAGTCTTGAA; *Tec*, forward GA TGGGAGTTACCAGTGTTGTAGACA and reverse GCGGGAGGCAGG GTCTT; *Rlk*, forward GCTGCTCAGTACAGAAGAGACAGG and reverse GAGTTTTGCCCATCAGTTTGG; *Bmx*, forward AAATTAAG AAAATCAGATGTGTGGAAAA and reverse CATTCGATGCATAGAC ATAAAGAAGC; and *Itk*, forward TTGAACTCTCCAGAATCAAGTG TGT and reverse ATAGTTGTCATGCACGACCTGTAAG.

### *Real-time PCR*

Real-time PCR was performed using the default PCR cycle on an ABI Prism 7900 HT Sequence Detection System (Applied Biosystems) and amplified DNA was detected by SYBR Green incorporation. Dissociation curve analyses were performed to confirm specificity of the SYBR Green signals in each experiment. Quantification of relative amounts of genes of interest was conducted using the Sequence Detection Systems Software (v.2.0; Applied Biosystems) and the comparative standard curve method, or the threshold cycle ($C_t$) method when the efficiency of primers were comparable. Data were normalized to the housekeeping gene hypoxanthine guanine phosphoribosyltransferase.

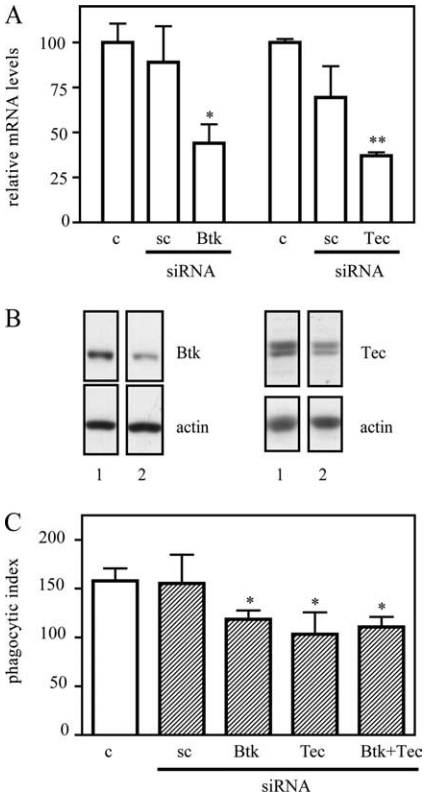


**FIGURE 1.** Silencing of *Btk* and *Tec* genes by siRNA. *A*, Real-time PCR was used to determine Btk and Tec mRNA expression levels in RAW cells transfected with or without the corresponding siRNA. For each kinase, mRNA levels were normalized to hypoxanthine guanine phosphoribosyltransferase and were compared with the corresponding values in untransfected controls (c), which were designated as 100. Data are expressed as mean ± SEM. sc, Scrambled control siRNA. **, $p < 0.001$; *, $p < 0.05$, relative to controls ($n$ = 2–4 experiments). *B*, Representative Western blots showing Btk and Tec protein expression levels in RAW cells transfected with scrambled (*lane 1*) or kinase (*lane 2*) siRNA. Comparable intensity of actin bands (*lane 1* vs *lane 2*) reflects equal protein loading. *C*, IgG-RBC phagocytosis was performed in RAW cells untransfected (c) or transfected with scrambled (sc), Btk, Tec, or Btk plus Tec siRNA. Phagocytic index is expressed as mean ± SEM from $n$ = 4–5 experiments. *, $p < 0.05$, relative to scrambled siRNA.

### *Statistical analysis*

Values correspond to mean ± SEM. In experiments with multiple groups, differences were first evaluated using one-way ANOVA, and Tukey-Kramer Multiple Comparison test was used to determine differences between pairs. Unpaired or paired Student's *t* tests were used when comparing differences between two groups.

## Results

### *RAW 264.7 cells express Btk and Tec*

Previous reports indicate that monocytes/macrophages express Btk, Tec and Bmx (22, 37). We investigated the mRNA expression for each Tec family kinase gene in RAW 264.7 mouse macrophage cell line (RAW cells) by real-time PCR (*Btk*, *Tec*, *Rlk*, and *Bmx*) or RT-PCR (*Itk*) using their respective primer pairs described earlier. In comparison to the expression of Tec family kinase genes in

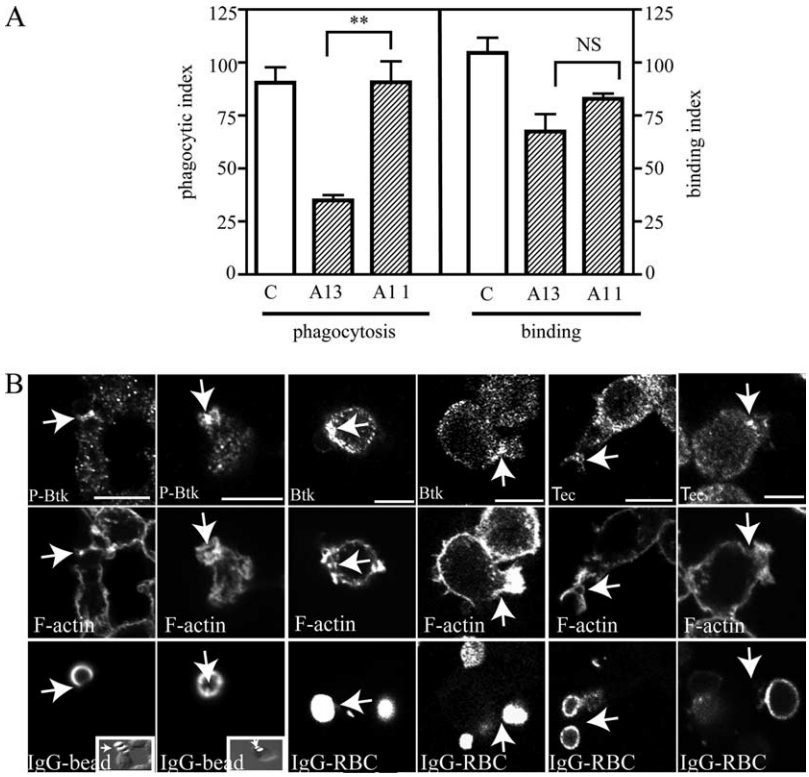


**FIGURE 2.** FcγR-mediated phagocytosis is dependent on Btk and Tec in RAW cells. *A*, Phagocytic index (*left*) and binding index (*right*) expressed as mean ± SEM in untreated cells (C) or cells pretreated with 100 μM LFM-A13 (A13) or 100 μM LFM-A11 (A11). **, $p < 0.001$, relative to LFM-A11 ($n = 4–5$ experiments). NS, Not significant. *B*, Endogenous phospho-Btk (P-Btk), Btk, and Tec accumulate at the phagocytic cup. Phagocytosis was initiated by addition of IgG-RBC or IgG-coated beads under conditions of binding assays. Cells were immunostained for phospho-Btk (P-BTK), Btk, or Tec (*upper*), F-actin (*middle*), and IgG (*lower*). Phagocytic cups were identified by F-actin and extracellular IgG-coated beads (for phospho-Btk) or IgG-RBC (for Btk and Tec). DIC images show all the beads (*inset*). Note that phospho-Btk, Btk, and Tec (*upper*) accumulated at the base of phagocytic cups (arrows) and do not colocalize precisely with F-actin (see arrows in the corresponding *lower panels*). Staining was not observed with nonimmune rabbit IgG or goat IgG (negative controls for phospho-Btk and Btk or Tec Abs, respectively). Scale bar represents 10 μm.

mouse splenocytes (*Btk*, *Tec*, *Rlk*, and *Itk*) and peritoneal macrophages (*Btk* and *Bmx*), Btk and Tec mRNA transcripts were readily detected in RAW cells, but the expression of *Itk*, *Rlk*, and *Bmx* genes was undetectable (data not shown). Expression of Btk and Tec protein in RAW cells was demonstrated by Western blotting and immunoprecipitation (described below).

### *Btk and Tec are required for optimal FcγR-mediated phagocytosis*

Having found that Btk and Tec are the major Tec family kinases expressed by RAW cells, we investigated their involvement in FcγR-induced phagocytosis. We studied the contribution of each kinase by inhibiting expression with siRNA. We obtained modest but consistent inhibition of expression only when a 2-day transfection protocol was used, as described in *Materials and Methods*. Fig. 1*A* shows significant reduction (50–60%) in Btk and Tec mRNA expression when targeted by the respective siRNA. The protein expression of Btk and Tec was reduced by 43 ± 10.2% and 27 ± 2.7%, respectively, relative to scrambled control siRNA ($n = 3$ experiments). Fig. 1*B* shows one representative blot. The phagocytic index in Btk or Tec siRNA transfectants was significantly lower than in untreated or scrambled RNA-transfected control cells (Fig. 1*C*). The extent of the reduction was consistent with the extent of silencing observed in protein expression described earlier. There was no additive effect when RAW cells were simultaneously transfected with Tec and Btk siRNAs, suggesting that the two kinases may function in the same pathway.

We also used LFM-A13, a known inhibitor of Tec family kinase activity, to test the requirements for Tec and Btk in FcγR-induced phagocytosis. LFM-A13 was described originally as an inhibitor of Btk, but was subsequently shown to inhibit other Tec family members, Tec and Bmx, in fMLP-induced neutrophils (23). LFM-A13 binds to the catalytic pocket of the kinase domain and does not inhibit other tyrosine kinases such as HCK, EGFR, Jak1, Jak3 (38, 39) with the exception of Jak2, which is involved in cytokine

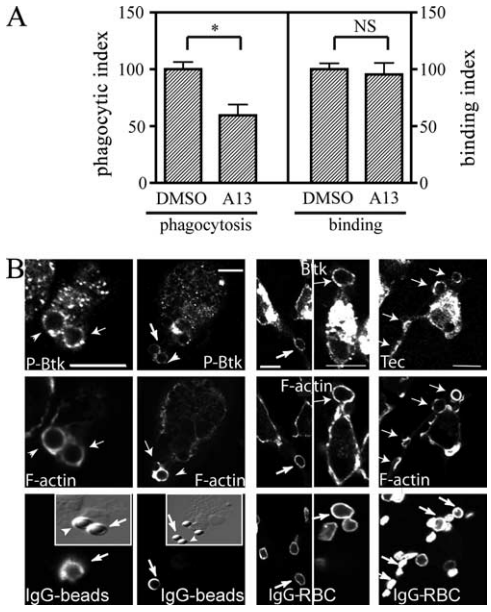


**FIGURE 3.** FcγR-mediated phagocytosis is dependent on Btk and Tec in peritoneal macrophages. *A*, Phagocytic (*left*) and binding (*right*) indices of peritoneal macrophages pretreated with DMSO (carrier) or 100 μM LFM-A13 (A13). Data are expressed as mean ± SEM and normalized to the respective value in DMSO. *, $p < 0.05$ ($n = 4$ mice). NS, Not significant. *B*, Endogenous phospho-Btk, Btk, and Tec accumulate at the phagocytic cup. Phagocytosis was initiated by the addition of IgG-RBC or IgG-coated beads under conditions of binding assays. Cells were fixed and immunostained for phospho-Btk, Btk, or Tec (*upper*), F-actin (*middle*), and IgG (*lower*). Focal accumulations of phospho-Btk or Btk and Tec in F-actin-rich phagocytic cups containing extracellular IgG-coated beads or IgG-RBC, respectively, are marked with arrows and in newly formed F-actin-rich phagosomes containing ingested beads, seen only in DIC images, (*inset*) with arrowheads in the *upper panels* and all corresponding *lower panels*. Staining was not observed with nonimmune rabbit IgG or goat IgG. Scale bar represents 10 μm.

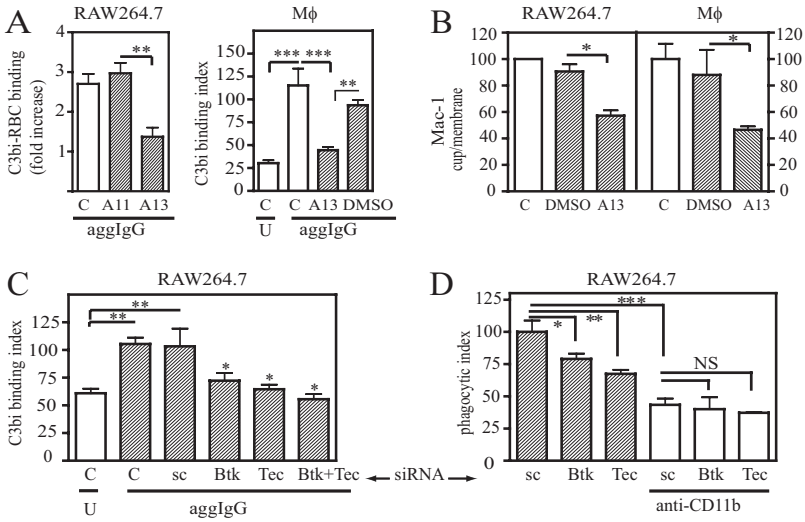


**FIGURE 4.** Btk and Tec are required for FcγR-induced activation of Mac-1. *A*, Unstimulated and aggIgG-stimulated (250 μg/ml) RAW cells and peritoneal macrophages (Mϕ) were exposed to C3bi-opsonized RBC for 20 min. C3bi binding values are mean ± SEM and are expressed as fold increase in aggIgG-stimulated relative to unstimulated RAW cells and as absolute values in unstimulated (U) and aggIgG-stimulated peritoneal macrophages. Effects of LFM-A13 (A13) were compared with that of LFM-A11 (A11) and carrier (DMSO) or no pretreatment (C). **, $p < 0.01$ relative to LFM-A11 or DMSO ($n = 4$ experiments); ***, $p < 0.001$ relative to no pretreatment (C) ($n = 4$ experiments). *B*, Mac-1 accumulation at phagocytic cups in RAW cells and peritoneal macrophages (Mϕ). IgG-RBC binding was initiated as in binding assays, Mac-1 was revealed by immunostaining, and pixel density at the cup vs adjacent membrane was determined. *, $p < 0.05$ relative to DMSO ($n = 3$ experiments). *C*, C3bi-opsonized RBC binding was determined as the mean ± SEM in unstimulated (U) or aggIgG-treated RAW cells transfected with siRNA. Cells were untransfected (C) or transfected with scrambled control (sc), Btk, Tec, or Btk plus Tec siRNA. *, $p < 0.05$ relative to scrambled siRNA or untransfected cells; **, $p < 0.01$ relative to unstimulated cells (U) ($n = 4–8$ experiments). *D*, The effects of Btk and Tec silencing on phagocytosis of IgG-RBC in the presence and absence of Mac-1 blocking in RAW cells. IgG-RBC phagocytosis was initiated in siRNA-transfected (scrambled control (sc), Btk, or Tec) cells that were pretreated with or without anti-CD11b (5 μg/ml) blocking Abs. *, $p < 0.05$; **, $p < 0.01$; ***, $p < 0.001$, relative to scrambled control siRNA-transfected cells without Mac-1 blockade ($n = 3–8$ experiments); NS, Not significant.

signaling (40). We compared the phagocytic index of the untreated RAW cells with those pretreated with LFM-A13 or the nonactive analog, LFM-A11 (Fig. 2*A*). There was a significant reduction in phagocytosis of IgG-RBC in cells pretreated with LFM-A13 relative to LFM-A11 pretreatment or no treatment. In contrast, we did not observe any significant effect of LFM-A13 on the extent of IgG-RBC binding as compared with LFM-A11, whereas a relatively small reduction was observed in comparison to no treatment. These findings indicate that Tec family kinase activity is required after binding of IgG-RBC to FcγR and clustering of the receptors. The kinase inhibitor results are consistent with data obtained using the siRNA approach and confirm that Btk and Tec are required for FcγR-mediated phagocytosis.

Activation of Btk and Tec requires binding to phosphatidylinositol 3,4,5-trisphosphate ($PIP_3$) and this phosphoinositide accumulates at the phagocytic cup within minutes of exposure to IgG-opsonized targets (33, 41, 42). Therefore, we investigated whether Btk and Tec are recruited to cups. Because active forms of Btk can be detected by phospho-specific Btk Abs, which recognize autophosphorylation at $Tyr^{223}$ of the Src homology 3 domain of Btk, we used these Abs to verify the accumulation of phosphorylated (active) phospho-Btk at phagocytic cups. Fig. 2*B* shows examples of endogenous Btk and Tec accumulating at phagocytic cups that are identified by staining for F-actin and IgG-RBC. Phospho-Btk, Btk, and Tec did not colocalize with F-actin but clustered at the base of the cup (Fig. 2*B*, open arrows). We repeated these experiments with elicited peritoneal macrophages to verify whether our findings in the RAW cell line can be expanded to primary macrophages. Fig. 3*A* shows that treatment with LFM-A13 resulted in a significant reduction in the levels of IgG-RBC phagocytosis, relative to control, whereas the binding of IgG-RBC was not affected. Control experiments were performed with the carrier DMSO, which yielded similar values to the untreated or LFM-A11-treated samples (data not shown). We also found marked accumulations of Btk, phospho-Btk, and Tec at phagocytic cups in peritoneal macrophages (Fig. 3*B*).

Immunostaining of phospho-Btk (rabbit IgG) at the cups was performed with cells phagocytosing human IgG-coated beads rather than IgG-RBC to avoid cross-reactivity of the anti-rabbit secondary Abs with RBC-opsonizing IgG. In these experiments (Figs. 2*B* and 3*B*), we detected the extracellularly bound beads by immunostaining for human IgG, whereas all the beads, including the ingested ones, were detected by DIC. We observed a rather prolonged accumulation of phospho-Btk during the ingestion of beads, for which examples are shown in Fig. 3*B*. Phospho-Btk was detected at the cups enriched with F-actin, containing extracellular IgG-coated beads (Fig. 3*B*, open arrows), and also in newly formed F-actin-rich phagosomes with ingested beads (Fig. 3*B*, arrowheads, and *inset*). Taken together, these results show that active forms of Btk and Tec accumulate at the cup and support our data with siRNA and LFM-A13, for a role of Btk and Tec in the ingestion of IgG-opsonized targets during FcγR-mediated phagocytosis.

### *Btk and Tec are involved in FcγR-mediated activation of Mac-1*

Previously, we reported that FcγR-induced activation of the integrin Mac-1 is required for optimal phagocytosis and we showed that FcγR signaling modulates the mobility of Mac-1 along the plasma membrane and leads to its accumulation at the phagocytic cup (32). Having found a role for Btk and Tec in FcγR-induced phagocytosis, we investigated whether they regulate FcγR-induced Mac-1 activation by assessing the binding of C3bi-opsonized RBC (Fig. 4). To this end, we used the inhibitor LFM-A13 or siRNA for

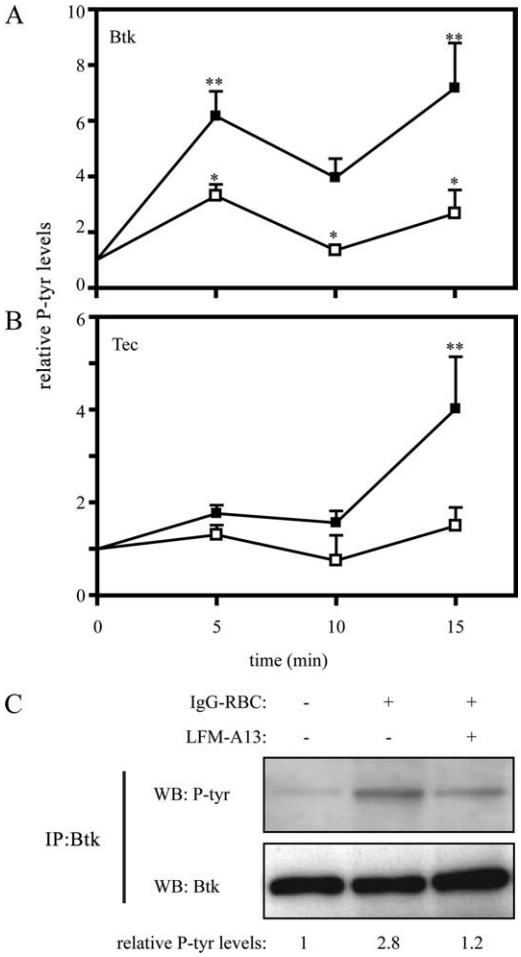


**FIGURE 5.** Kinetics of Btk and Tec activation induced by FcγR signaling. RAW cells without (■) or with (□) LFM-A13 pretreatment were incubated with IgG-RBC for 0, 5, 10, or 15 min. Phosphotyrosine (P-tyr) levels of Btk (*A*) and Tec (*B*) were analyzed by immunoprecipitation (IP) and Western blotting (WB) as shown in *C*. For each time point, phosphotyrosine levels were normalized to the abundance of total kinase and compared with values obtained in unstimulated cells (0 min, relative phosphotyrosine levels). **, $p < 0.01$, relative to unstimulated cells. Significant reductions by LFM-A13 pretreatment relative to untreated RAW cells at the corresponding time point are indicated. *, $p < 0.05$, $n = 3$–7 experiments. *C*, A typical analysis of a Btk immunoprecipitation by Western blot analysis performed 10 min poststimulation with IgG-RBC in the absence or presence of 100 μM LFM-A13. The number under each lane corresponds to relative phosphotyrosine levels.

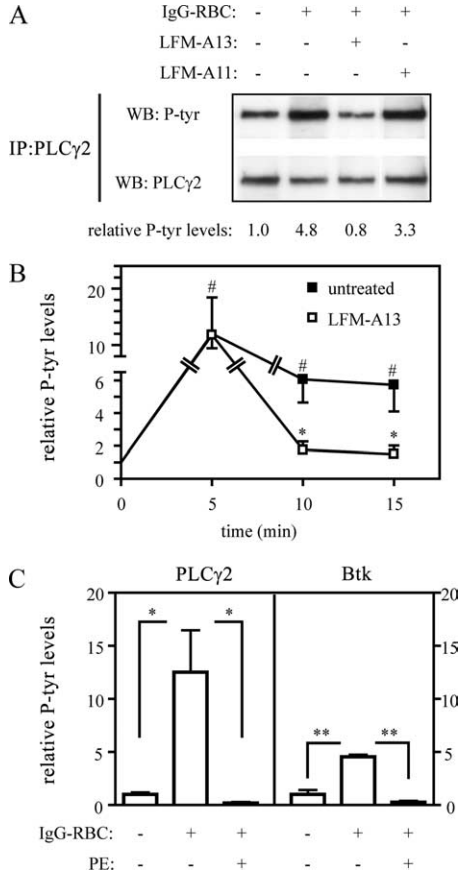


**FIGURE 6.** Tec family kinases mediate prolonged, but not early, activation of PLCγ2 induced by FcγR signaling. Immunoprecipitation (IP) of PLCγ2 was performed at different times after stimulation of RAW cells by IgG-RBC. *A*, A representative Western blot (WB) shows PLCγ2 tyrosine phosphorylation (P-tyr) and expression levels. Stimulation for 10 min with IgG-RBC and pretreatment with LFM-A13 (100 μM) or LFM-A11 (100 μM) are indicated above each lane. The number below each lane corresponds to the ratio of phosphotyrosine to total PLCγ2 normalized to the lane that was not treated with IgG-RBC (relative phosphotyrosine levels). Note that the marked increase in phosphotyrosine induced by IgG-RBC treatment at 10 min is completely inhibited by LFM-A13, but not LFM-A11. *B*, The time course of PLCγ2 activation (relative phosphotyrosine levels) after stimulation with IgG-RBC is shown. Each data point represents the mean ± SEM of $n = 3$–9 experiments such as the one shown in *A*. RAW cells were untreated or pretreated with LFM-A13 (100 μM) as indicated. Significant increases in relative phosphotyrosine were found at all time points #, $p < 0.05$. Note that LFM-A13 inhibited PLCγ2 phosphotyrosine at 10 and 15 min, but not 5 min. *, $p < 0.05$ relative to the corresponding time point. *C*, Effects of piceatannol (PE, 50 μM) on PLCγ2 and Btk relative phosphotyrosine levels determined by immunoprecipitation and Western blot analysis, 5 min after stimulation with IgG-RBC. IgG-RBC induced a marked increase in both PLCγ2 and Btk phosphotyrosine levels, which was completely inhibited by piceatannol. *, $p < 0.05$; **, $p < 0.01$ from $n = 3$ experiments.

Btk and Tec. Preincubation of RAW cells with LFM-A13 significantly inhibited aggIgG-induced binding of C3bi-opsonized RBC in RAW cells and in peritoneal macrophages (Fig. 4*A*). FcγR-induced Mac-1 activation is dependent on PLCγ and novel PKC (32). We found that PMA-induced activation of Mac-1 was not affected by LFM-A13 in RAW cells (data not shown), indicating that Tec kinases function upstream of PKC. In support of a role for these kinases in Mac-1 activation, we also observed that LFM-A13 treatment resulted in a significant decrease in Mac-1 accumulation at the cup during IgG-RBC ingestion in RAW cells and peritoneal macrophages (Fig. 4*B*). Transfection of RAW cells with Btk or Tec siRNA or with both also yielded a significant reduction in Mac-1 activation (Fig. 4*C*), in fact close to the resting levels. Because only partial silencing of Btk and Tec expression is achieved by the siRNA (Fig. 1, *A* and *B*), these data suggest a major role for Btk and Tec in FcγR-induced Mac-1 activation. These findings prompted us to ask whether the primary role of Tec family kinases in FcγR-mediated phagocytosis is to modulate Mac-1 activity. We tested this possibility by assessing the effects of Btk and Tec siRNA on phagocytosis when Mac-1 binding to ligand was blocked by CD11b blocking mAbs (Fig. 4*D*). We previously showed that blocking Mac-1 reduces the extent of IgG-RBC phagocytosis (32). Consistent with these data, in RAW cells transfected with control scrambled siRNA, the phagocytic index was reduced significantly by blocking Mac-1 (Fig. 4*D*). Targeting of Btk or Tec with siRNA did not reduce phagocytosis further under

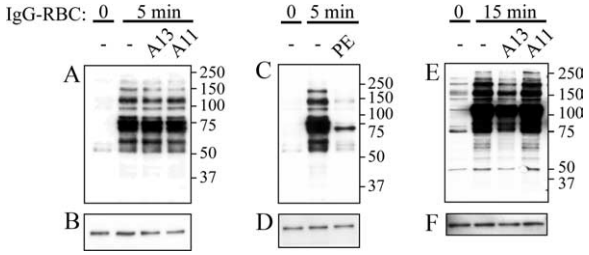


**FIGURE 7.** FcγR-induced tyrosine phosphorylation of cellular proteins by Tec family kinases at late stages of phagocytosis. Cells were incubated in the absence (0 min) or presence of IgG-RBC for 5 min (*A–D*) or 15 min (*E* and *F*). Lysates with equal protein amounts were analyzed by Western blotting for phosphotyrosine (P-tyr) (*A*, *C*, and *E*) in cells preincubated without (−) or with 100 μM LFM-A13 (A13), 100 μM LFM-A11 (A11), or 50 μM piceatannol (PE). Equal protein loads are shown (*B*, *D*, and *F*) using the same blots as in *A*, *C*, and *E*, reprobed for PLCγ2 (*B* and *D*) or Btk (*F*).

conditions of Mac-1 blockade, in contrast to cells treated without blocking Abs (Fig. 4*D*) or with rat IgG2b (isotype control for anti-CD11b; data not shown). These data suggest strongly that the effects of Btk or Tec on IgG-RBC phagocytosis is dependent on their role in Mac-1 activation.

### *Kinetics of activation of Btk and Tec by FcγR signaling*

Tec family kinases assume a fully active configuration after tyrosine phosphorylation by other kinases (Src, Syk) and autophosphorylation (20, 28, 43). Therefore, the level of tyrosine phosphorylation directly reflects the extent of activation and this approach was used to investigate the kinetics of Btk and Tec activation in RAW cells stimulated with IgG-RBC. Immunoprecipitation of the respective kinase was performed at different times after stimulation (0–15 min), followed by Western blotting for phosphotyrosine (Fig. 5). We observed a marked increase in the activation of Btk at 5, 10, and 15 min (Fig. 5, *A* and *C*). Pretreatment with LFM-A13 significantly reduced Btk activation at all time points tested, consistent with the notion that active kinases undergo autophosphorylation. The kinetics of Tec activation appeared different. There was a small increase at 5 and 10 min and a significant elevation at 15 min (Fig. 5*B*). Tec activation was inhibited by LFM-A13. The activation of Btk and Tec was not affected by LFM-A11 (data not shown). These data show that Btk and to a lesser extent Tec are activated within 5 min, concurrent with their accumulation at phagocytic cups (Fig. 2*B*), and these kinases remain active at later stages of phagocytosis, when phagosome formation and maturation occur.

### *Requirement for Btk and Tec in downstream signaling during late stages of phagocytosis*

PLCγ is one of the targets of Tec kinases. Because PLCγ2 is expressed at higher levels than PLCγ1 in RAW cells (19), we investigated the role of Tec family kinases in PLCγ2 activation in these cells stimulated by IgG-RBC (Fig. 6). PLCγ2 phosphorylation showed a 12-fold increase over control levels at 5 min and remained elevated (6-fold or higher) at 10 and 15 min (Fig. 6, *A* and *B*). Pretreatment with LFM-A13 inhibited PLCγ2 phosphorylation at 10 and 15 min, but not at 5 min. Because tyrosine phosphorylation of PLCγ has been associated with its activation (44), these results suggest that Tec family kinases regulate PLCγ2 activation at late stages of FcγR-mediated phagocytosis. Regulation of PLCγ2 activity by Syk has been described during Ag receptor signaling (45) thus, we investigated its role in FcγR-induced signaling. Fig. 6*C* shows that pretreatment of RAW cells with the Syk inhibitor piceatannol inhibited tyrosine phosphorylation of PLCγ2 at 5 min. Similarly, tyrosine phosphorylation of Btk was also inhibited by piceatannol under the same conditions. These data indicate that Syk is critical in initiating the activation of PLCγ2 and Btk.

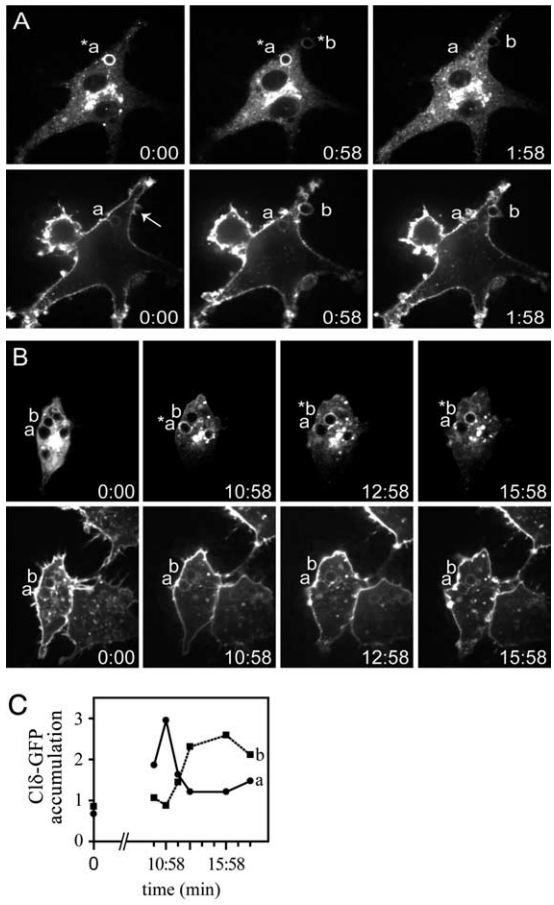


**FIGURE 8.** Accumulation of DAG in phagosome membranes. *A* and *B*, Representative data from live cell imaging studies are shown. PKC C1δ-GFP accumulation in phagosomes of transfected RAW cells (*top*) and phagosome and plasma membranes stained with cholera toxin B (*bottom*) are shown. Phagosomes with accumulated C1δ-GFP are designated (a or b). The number in each panel corresponds to time point (min:sec) and is relative to the start of recording (0:00), which is not necessarily the beginning of ingestion. Asterisk denotes phagosomes with accumulated C1δ-GFP. *A*, Cell with an abundant accumulation of C1δ-GFP in a phagosome membrane (designated a) is shown. Accumulation persisted at 0:58, but was markedly reduced at 1:58. A newly formed cup (arrow) is depicted at 0:00 (*bottom panel*). It matured into a phagosome (designated b) at 0:58, and C1δ-GFP accumulation is detected transiently at this time. At 1:58 accumulation is diminished. *B*, Transient (designated a) and more persistent (designated b) accumulation of PKC C1δ-GFP is depicted. Both phagosomes were present from the start of recording (determined by cholera toxin B staining). A transient accumulation of PKC C1δ-GFP was observed in phagosome a at 10:58, whereas persistent maximal accumulation was found in phagosome b starting at 12:58. *C*, Quantification of the time course of C1δ-GFP accumulation in phagosomes (a and b) from *B* is shown. GFP signal pixel density in phagosomes relative to the adjacent cytosol is plotted. Tick lines represent time points shown in the images.

The dichotomy observed between Syk and Tec kinases to activate PLCγ2 may be unique or may reflect the functioning of these two types of kinases on a broader spectrum of proteins during FcγR-induced phagocytosis. To test these possibilities, we assessed the overall tyrosine phosphorylation of cellular proteins at different times of stimulation with IgG-RBC in the presence of LFM-A13 or piceatannol. Fig. 7 shows that LFM-A13 did not

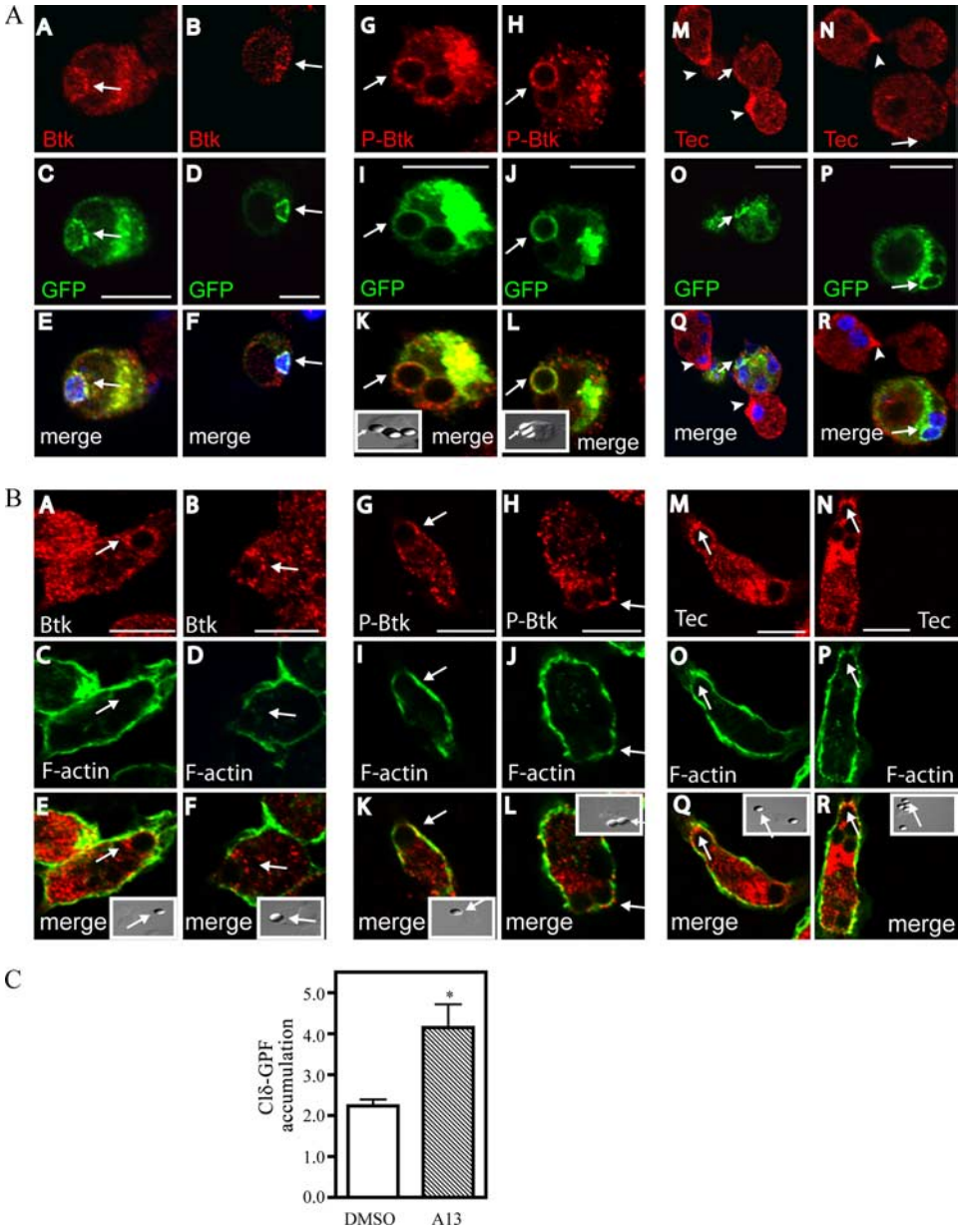


**FIGURE 9.** Btk, but not Tec, accumulates in phagosomes. *A*, RAW cells transfected with PKC C1δ-GFP were incubated with IgG-RBC or IgG-coated beads for 20–25 min and fixed cells were immunostained for endogenous Btk, phospho-Btk (P-Btk), or Tec and IgG (extracellular for beads). Panels A,B, G,H, and M,N show Btk, phospho-Btk (arrows), and Tec (arrowhead) accumulation, respectively. Panels C,D, I,J, and O,P show PKC C1δ-GFP accumulation (arrows) in the phagosomes of transfected cells in the fields that correspond to the *upper panels*. IgG-RBC or IgG-coated beads in phagosomes are shown in merged images in blue (E, F and Q, R) or in DIC images (K, L) (*inset*), respectively, in the *lower panels*. Note that staining for Btk, phospho-Btk, and PKC C1δ-GFP colocalizes in the phagosome membranes (arrows in panels E,F and K,L). Arrows in M,N denote the location of PKC C1δ-GFP$^+$ phagosomes detected in transfectants in panels O,P, respectively, and Tec does not accumulate around these phagosomes (Q,R) but in clusters at sites of phagosome formation (arrowheads). Scale bar represents 10 μm. *B*, Peritoneal macrophages were incubated with IgG-coated beads and analyzed for Btk, phospho-Btk, and Tec (arrows) (*upper*) and for F-actin (*middle*). Panels A,B and G,H show examples of Btk and phospho-Btk accumulation, respectively, and panels M,N show Tec clustering (arrows). Ingested beads imaged by DIC (*inset*) did not stain extracellularly for IgG. *Panels C–F* and *I–L* show that Btk and phospho-Btk, respectively, accumulated around phagosomes in which F-actin is not enriched. Panels O–R show Tec clustering (arrows) at sites of phagosome formation that did not colocalize with F-actin. Scale bar represents 10 μm. *C*, PKC C1δ-GFP-transfected RAW cells were pretreated with carrier (DMSO) or 100 μM LFM-A13 (A13) and phagocytosis of IgG-RBC proceeded for 25 min. Pixel density of GFP in phagosomes vs cytosol was determined in 15–30 cells per experiment. ∗, $p < 0.05$ ($n = 3$ experiments).

affect the bulk of tyrosine phosphorylation at 5 min of stimulation as opposed to a significant inhibition by piceatannol (Fig. 7, *A* and *C*). However, at 15 min of stimulation we detected a marked reduction in phosphotyrosine levels of a number of proteins (Fig. 7*E*) in LFM-A13- but not LFM-A11-treated cells. Similar results were observed at 10 min (data not shown). Taken together, these results show that Syk regulates tyrosine phosphorylation of several proteins (including PLCγ2 and Btk) at 5 min of phagocytosis (Fig. 6*C*), whereas activated Tec kinases likely modulate a limited number of effectors. In contrast, Tec family kinases modulate the phosphorylation of PLCγ2 and a number of other potential effectors at later stages of FcγR-mediated phagocytosis (Fig. 6*B*).

*Accumulation of DAG and Btk in phagosome membranes*

A previous study by Botelho et al. (15) described the accumulation of PLCγ2 at the phagocytic cup. This event is dependent on Syk and is independent of Tec family kinases (Fig. 6). Because we found that Btk and Tec are necessary for maintaining PLCγ2 activity at or beyond 10 min, which coincides with the maturation of phagosomes, we investigated whether DAG, a product of PLCγ, accumulates in phagosomes. RAW cells were transfected with the PKC C1δ-GFP cDNA, which encodes a fusion protein consisting of GFP and the C1 domain of PKCδ that binds effectively to DAG (46). Phagosomes were visualized in live cells by cholera toxin B, which stains cellular membranes (35), and in fixed cells by staining for IgG on ingested IgG-RBC. In fixed cells, GFP was enriched in 27.8 ± 3.1% ($n$ = 4 experiments) of phagosomes at 10–25 min. This rate reflects the transient nature of accumulation and a heterogeneity among the phagosomes that is apparent by live cell imaging experiments (Fig. 8, *A* and *B*). Although most phagosomes displayed transient accumulation of GFP (Fig. 8*A*, see phagosomes a and b and phagosome a in Fig. 8, *B* and *C*), we also detected phagosomes that accumulated GFP for relatively longer periods of time (Fig. 8, *B* and *C*, see phagosome b). These observations of C1δ-GFP accumulation in phagosomes are novel and implicate PLCγ activation, accumulation of DAG, and potential activation of DAG-binding proteins such as PKC and guanine nucleotide exchange factor GEF. The time frame for the generation of DAG in phagosome membranes correlated with tyrosine phosphorylation of PLCγ2, which was dependent on Tec family kinases (see Fig. 6). Therefore, we investigated whether Tec family kinases accumulate at or near DAG-positive phagosomes. In PKCδC1-GFP transfectants, Btk was colocalized with GFP (DAG) in phagosome membranes, as was phospho-Btk (Fig. 9*A*, panels A–F and G–L, respectively). Quantitative analysis showed that 71.5 ± 4.1% of $DAG^+$ phagosomes were Btk-positive ($n$ = 4 experiments) and ~79% of DAG-positive phagosomes were phospho-Btk-positive. Tec, in contrast, was not found in phagosomes, but was clustered adjacent to the plasma membrane near phagosomes (Fig. 9*A*, panels M–R). These results suggest an active role for Btk in the accumulation of DAG, whereas Tec may have a different function during phagosome formation or maturation. We could not transfect peritoneal macrophages, but immunostaining studies in these cells showed similar accumulation patterns of Tec family kinases at or near IgG bead-containing phagosomes, i.e., Btk and phospho-Btk were seen in phagosome membranes and Tec was at sites of phagosome formation (Fig. 9*B*), suggesting that Btk and Tec have distinct functions in both primary macrophages and in RAW cells. To get an insight whether Btk activity modulates DAG levels in phagosomal membranes, we took advantage of the fact that LFM-A13 inhibited phagocytosis partially (see Figs. 2 and 3) and determined its effect on PKCδC1-GFP accumulation. Fig. 9*C* shows that GFP levels in phagosome membranes increased by close to 2-fold in the presence of LFM-A13. This unexpected finding suggests a negative regulatory role for Btk in PKCδC1-GFP (DAG) accumulation in phagosomes.

## Discussion

Tec family kinases are widely expressed in the myeloid lineage and are coupled to a variety of receptors, including G protein-coupled receptors, TLRs, and integrins, thus they may participate in multiple cellular functions (22). The involvement of Btk in FcγR-mediated phagocytosis has previously been reported in monocytes from patients with XLA (25) and in peritoneal macrophages from xid mice that have a mutation in the *btk* gene (47). These studies did not investigate the mode of Btk functioning or the participation of other Tec family members in phagocytosis. In this study, we showed that Btk and Tec are required for optimal FcγR-mediated phagocytosis in RAW cells and we confirmed this role of Tec family kinases in primary peritoneal macrophages. Our data point to two stages of FcγR-mediated phagocytosis in which Tec kinases are implicated: ingestion and at later stages when phagosomes are formed and mature. We demonstrated the activation of Btk and Tec by two different approaches: phosphorylation of the immunoprecipitated kinases, measuring overall cellular activity, and accumulation in cell membranes, indicating local activity. The first stage for Btk and Tec activation is within 5 min, downstream of Syk, when nascent phagosomes (cups) are formed. Although the overall Btk activation was more prominent than Tec at this stage (Fig. 5), we found the accumulation of both kinases, including autophosphorylated active Btk (phospho-Btk), at phagocytic cups. These findings are consistent with a previous report of a fusion protein of the pleckstrin homology domain of Btk linked to GFP (Btk-PH-GFP) accumulating at phagocytic cups (42). The activation of Btk and Tec is initiated by their recruitment to the membrane through binding of their N-terminal pleckstrin homology domain to $PIP_3$, a product of PI3K (48). Consistent with this, Btk translocations into areas of PI3K activation and dynamic membrane and cytokeleton remodeling were demonstrated (33). In additon, Btk and Tec were recruited to immunological synapses where active actin remodelings take place in APCs (49–51). It is likely that Btk and Tec participate in the active reorganization of actin-cytoskeleton at the cup, where the PI3K product $PIP_3$ accumulates (42, 52). One of the events accompanying cup formation is the activation of Mac-1, which is required for optimal phagocytosis. FcγR signaling induces the transition of the integrin from a cytoskeleton-bound resting to a mobile state, which results in clustering of Mac-1 at phagocytic cups and binding to ligand (32). Both PI3K and PLCγ activity mediate FcγR-induced Mac-1 activation, and we showed that Btk and Tec are also involved (Fig. 4, *A–C*). In fact, we showed that the roles of Btk and Tec in Mac-1 activation are related to their functions during the ingestion of IgG-RBC because targeting of these kinases by siRNA inhibited phagocytosis only when Mac-1 was functional (Fig. 4*D*). The accumulation of phospho-Btk and Tec (data not shown) persisted over the process of phagosome sealing when F-actin enrichment around the newly formed phagosome was still apparent before its depolymerization (Fig. 3*B*) (52), as was described for Syk and PI3K (42).

Botelho et al. (7, 15) showed a transient early accumulation of the PLCγ product DAG at the base of phagocytic cups and similarly, we observed the recruitment of active Btk and Tec to the base of cups away from pseudopods, where F-actin is enriched. Although a role for PLCγ2 in cup formation was questioned, PLCγ2 accumulates in sealing phagosomes during the uptake of IgG-RBC (7) and the robust activation of PLCγ2 that we found at 5 min of stimulation supports a role for this enzyme in FcγR signaling. However, we did not detect a role for Tec kinases in the activation of PLCγ2 or tyrosine phosphorylation of most cellular proteins at early stages of phagocytosis, indicating that the activities of Btk and Tec influence the functioning of a narrow range of effectors involved in cup formation. Cheeseman et al. (19) recently showed a transient early accumulation of active PLCγ1 and its importance in cup formation. It is possible that the early activation of Tec kinases is important for FcγR-induced PLCγ1 activation. In support of this possibility and a role in cup formation, the actin-organizing molecule WASP, which interacts with Btk (53, 54), and SLP-76, the adaptor protein coupling Tec kinases to the activation of PLCγ in T cells (55), are found in phagocytic cups in RAW cells (56).

Tec is functional in platelets from patients with XLA (27) and it has redundant function with Btk in B cell development and activation (57). These findings raise the question whether Btk and Tec functions are redundant during the uptake of IgG-opsonized particles. Our observations of cells treated with Btk and Tec siRNA, simultaneously (Figs. 1*C* and 4*C*), do not support the possibility of compensatory mechanisms between the two enzymes, but rather suggest that their activities depend on each other. We obtained partial inhibition of phagocytosis with LFM-A13 and limited extent of inhibition of Fc$\gamma$R-induced overall tyrosine phosphorylation with this inhibitor relative to the profound inhibition by the Syk inhibitor, piceatannol, suggestive of a modulatory function of these kinases during phagocytosis, similar to their previously described role in Ag receptor signaling (58).

The persistent activation of Btk at 10 or 15 min and the elevated activation of Tec at 15 min suggest a second wave of Tec family kinase involvement that likely coincides with phagosome maturation (59, 60). Future studies will determine the precise stage of maturation in which these kinases function by using specific maturation markers. PLC$\gamma$2 activity also remains elevated and Tec family kinases are required for this late activity as well as the tyrosine phosphorylation of a number of cellular proteins. A previous study showed the presence of $PIP_2$, the substrate for PLC, in purified latex bead phagosomes (61). We demonstrated the accumulation of the PKC$\delta$C1-GFP probe in a significant number of phagosomes at 15–25 min after the initiation of phagocytosis. To our knowledge, these data are the first to implicate PLC activation and DAG accumulation at this stage of phagocytosis. It is possible that the strong interaction of the PKC$\delta$C1-GFP probe with DAG may have stabilized DAG and facilitated its detection in phagosome membranes. Alternative approaches to detect DAG will be needed to assess levels in phagosomes. DAG is bound by C1 domains of signaling molecules, such as the conventional and novel PKCs and *ras*-GRP, which is a novel *ras*-guanine nucleotide exchange factor that contains a DAG binding domain (62, 63). The target proteins of phagosomal DAG and their role in phagosome maturation remain to be identified. Because Tec family kinases remain active even at 15 min after the initiation of phagocytosis, we predicted that Btk and Tec may participate in the accumulation of DAG in phagosomes. We found enrichment of catalytically active Btk in the majority of phagosomes with accumulated PKC$\delta$C1-GFP, suggesting that Btk may contribute to DAG accumulation. Tec, however, was not present on phagosomes. LFM-A13 experiments suggest a negative regulatory function for Btk in DAG accumulation (Fig. 9*C*). Because DAG kinases convert DAG into phosphatidic acid and regulate membrane DAG levels (64, 65), it is conceivable that Btk activates DAG kinase in phagosome membranes. These data suggest that DAG formation in phagosomes is not mediated by Tec family kinase-dependent PLC$\gamma$2 activity. The demonstration of Tec clustering at sites of phagosome formation (Fig. 9, *A* and *B*) suggests that Tec may be involved in phagosome scission or targeting to the endocytic pathway for maturation. Whether PLC$\gamma$2 is a target for Tec in mediating such function remains to be elucidated. The distinct distribution patterns of Btk and Tec at relatively late stages of phagocytosis suggest unique downstream targets and functions, in contrast to the early uptake stage, at which the two kinases likely function in the same pathway. In summary, the modes of Btk and Tec activation and function appear to be complex and differ between the ingestion and maturation stages of Fc$\gamma$R-mediated phagocytosis.

## Acknowledgments

We are indebted to Dr. Sergio Grinstein for valuable advice and for providing the PKC$\delta$-C1GFP cDNA construct. We thank Paul Paroutis at the Imaging Facility of the Hospital for Sick Children Research Institute for his help with live cell imaging and Mark Hewshue and Dr. Mian Chen for assistance with PCR experiments. We also thank Dr. Rene Harrison for critical reading of the manuscript.

## Disclosures

The authors have no financial conflict of interest.

## References

1. Greenberg, S., and S. Grinstein. 2002. Phagocytosis and innate immunity. *Curr. Opin. Immunol.* 14: 136–145.
2. Kwiatkowska, K., and A. Sobota. 1999. Signaling pathways in phagocytosis. *Bioessays* 21: 422–431.
3. Greenberg, S. 1999. Modular components of phagocytosis. *J. Leukocyte Biol.* 66: 712–717.
4. Swanson, J. A., and S. C. Baer. 1995. Phagocytosis by zippers and triggers. *Trends Cell Biol.* 5: 89–93.
5. Swanson, J. A., M. T. Johnson, K. Beningo, P. Post, M. Mooseker, and N. Araki. 1999. A contractile activity that closes phagosomes in macrophages. *J. Cell Sci.* 112: 307–316.
6. Niedergang, F., and P. Chavrier. 2004. Signaling and membrane dynamics during phagocytosis: many roads lead to the phagos(R)ome. *Curr. Opin. Cell Biol.* 16: 422–428.
7. Botelho, R. J., C. C. Scott, and S. Grinstein. 2004. Phosphoinositide involvement in phagocytosis and phagosome maturation. *Curr. Top. Microbiol. Immunol.* 282: 1–30.
8. Kim, M. K., X. Q. Pan, Z. Y. Huang, S. Hunter, P. H. Hwang, Z. K. Indik, and A. D. Schreiber. 2001. Fc$\gamma$ receptors differ in their structural requirements for interaction with the tyrosine kinase Syk in the initial steps of signaling for phagocytosis. *Clin. Immunol.* 98: 125–132.
9. Raeder, E. M., P. J. Mansfield, V. Hinkovska-Galcheva, J. A. Shayman, and L. A. Boxer. 1999. Syk activation initiates downstream signaling events during human polymorphonuclear leukocyte phagocytosis. *J. Immunol.* 163: 6785–6793.
10. Crowley, M. T., P. S. Costello, C. J. Fitzer-Attas, M. Turner, F. Meng, C. Lowell, V. L. Tybulewicz, and A. L. DeFranco. 1997. A critical role for Syk in signal transduction and phagocytosis mediated by Fc$\gamma$ receptors on macrophages. *J. Exp. Med.* 186: 1027–1039.
11. Strzelecka-Kiliszek, A., K. Kwiatkowska, and A. Sobota. 2002. Lyn and Syk kinases are sequentially engaged in phagocytosis mediated by Fc$\gamma$R. *J. Immunol.* 169: 6787–6794.
12. Coppolino, M. G., R. Dierckman, J. Loijens, R. F. Collins, M. Pouladi, J. Jongstra-Bilen, A. D. Schreiber, W. S. Trimble, R. Anderson, and S. Grinstein. 2002. Inhibition of phosphatidylinositol-4-phosphate 5-kinase I$\alpha$ impairs localized actin remodeling and suppresses phagocytosis. *J. Biol. Chem.* 277: 43849–43857.
13. Zhang, Q., D. Cox, C.-C. Tseng, J. G. Donaldson, and S. Greenberg. 1998. A requirement for ARF6 in Fc$\gamma$ receptor-mediated phagocytosis in macrophages. *J. Biol. Chem.* 273: 19977–19981.
14. Hackam, D. J., O. D. Rotstein, A. Schreiber, W. Zhang, and S. Grinstein. 1997. Rho is required for the initiation of calcium signaling and phagocytosis by Fc$\gamma$ receptors in macrophages. *J. Exp. Med.* 186: 955–966.
15. Botelho, R. J., M. Teruel, R. Dierckman, R. Anderson, A. Wells, J. D. York, T. Meyer, and S. Grinstein. 2000. Localized biphasic changes in phosphatidylinositol-4,5-bisphosphate at sites of phagocytosis. *J. Cell Biol.* 151: 1353–1368.
16. Iyer, S. S., J. A. Barton, S. Bourgoin, and D. J. Kusner. 2004. Phospholipases D1 and D2 coordinately regulate macrophage phagocytosis. *J. Immunol.* 173: 2615–2623.
17. Lennartz, M. R. 1999. Phospholipases and phagocytosis: the role of phospholipid-derived second messengers in phagocytosis. *Int. J. Biochem. Cell Biol.* 31: 415–430.
18. Larsen, E. C., T. Ueyama, P. M. Brannock, Y. Shirai, N. Saito, C. Larsson, D. Loegering, P. B. Weber, and M. R. Lennartz. 2002. A role for PKC-$\varepsilon$ in Fc$\gamma$R-mediated phagocytosis by RAW 264.7 cells. *J. Cell Biol.* 159: 939–944.
19. Cheeseman, K. L., T. Ueyama, T. M. Michaud, K. Kashiwagi, D. Wang, L. A. Flax, Y. Shirai, D. J. Loegering, N. Saito, and M. R. Lennartz. 2006. Targeting of protein kinase C-$\varepsilon$ during Fc$\gamma$ receptor-dependent phagocytosis requires the $\varepsilon$C1B domain and phospholipase C-$\gamma$1. *Mol. Biol. Cell* 17: 799–813.
20. Smith, C. I., T. C. Islam, P. T. Mattsson, A. J. Mohamed, B. F. Nore, and M. Vihinen. 2001. The Tec family of cytoplasmic tyrosine kinases: mammalian Btk, Bmx, Itk, Tec, Txk and homologs in other species. *Bioessays* 23: 436–446.
21. Lindvall, J. M., K. E. Blomberg, J. Väliaho, L. Vargas, J. E. Heinonen, A. Berglöf, A. J. Mohamed, B. F. Nore, M. Vihinen, and C. I. Smith. 2005. Bruton's tyrosine kinase: cell biology, sequence conservation, mutation spectrum, siRNA modifications, and expression profiling. *Immunol. Rev.* 203: 200–215.
22. Schmidt, U., N. Boucheron, B. Unger, and W. Ellmeier. 2004. The role of Tec family kinases in myeloid cells. *Int. Arch. Allergy Immunol.* 134: 65–78.
23. Gilbert, C., S. Levasseur, P. Desaulniers, A. A. Dusseault, N. Thibault, S. G. Bourgoin, and P. H. Naccache. 2003. Chemotactic factor-induced recruitment and activation of Tec family kinases in human neutrophils. II. Effects of LFM-A13, a specific Btk inhibitor. *J. Immunol.* 170: 5235–5243.
24. Fernandes, M. J., G. Lachance, G. Paré, E. Rollet-Labelle, and P. H. Naccache. 2005. Signaling through CD16b in human neutrophils involves the Tec family of tyrosine kinases. *J. Leukocyte Biol.* 78: 524–532.

25. Amoras, A. L., H. Kanegane, T. Miyawaki, and M. M. Vilela. 2003. Defective Fc-, CR1- and CR3-mediated monocyte phagocytosis and chemotaxis in common variable immunodeficiency and X-linked agammaglobulinemia patients. *J. Investig. Allergol. Clin. Immunol.* 13: 181–188.
26. Valiaho, J., C. I. Smith, and M. Vihinen. 2006. BTKbase: the mutation database for X-linked agammaglobulinemia. *Hum. Mutat.* 27: 1209–1217.
27. Oda, A., Y. Ikeda, H. D. Ochs, B. J. Druker, K. Ozaki, M. Handa, T. Ariga, Y. Sakiyama, O. N. Witte, and M. I. Wahl. 2000. Rapid tyrosine phosphorylation and activation of Bruton's tyrosine/Tec kinases in platelets induced by collagen binding or CD32 cross-linking. *Blood* 95: 1663–1670.
28. Miller, A. T., and L. J. Berg. 2002. New insights into the regulation and functions of Tec family tyrosine kinases in the immune system. *Curr. Opin. Immunol.* 14: 331–340.
29. Takesono, A., L. D. Finkelstein, and P. L. Schwartzberg. 2002. Beyond calcium: new signaling pathways for Tec family kinases. *J. Cell Sci.* 115: 3039–3048.
30. Bonilla, F. A., R. M. Fujita, V. I. Pivniouk, A. C. Chan, and R. S. Geha. 2000. Adapter proteins SLP-76 and BLNK both are expressed by murine macrophages and are linked to signaling via Fcγ receptors I and II/III. *Proc. Natl. Acad. Sci. USA* 97: 1725–1730.
31. Wen, R., S. T. Jou, Y. Chen, A. Hoffmeyer, and D. Wang. 2002. Phospholipase Cγ2 is essential for specific functions of FcεR and FcγR. *J. Immunol.* 169: 6743–6752.
32. Jongstra-Bilen, J., R. Harrison, and S. Grinstein. 2003. Fcγ-receptors induce Mac-1 (CD11b/CD18) mobilization and accumulation in the phagocytic cup for optimal phagocytosis. *J. Biol. Chem.* 278: 45720–45729.
33. Nore, B. F., L. Vargas, A. J. Mohamed, L. J. Brandén, C. M. Bäckesjö, T. C. Islam, P. T. Mattsson, K. Hultenby, B. Christensson, and C. I. Smith. 2000. Redistribution of Bruton's tyrosine kinase by activation of phosphatidylinositol 3-kinase and Rho-family GTPases. *Eur. J. Immunol.* 30: 145–154.
34. Wang, C., H. Hayashi, R. Harrison, B. Chiu, J. R. Chan, H. L. Ostergaard, R. D. Inman, J. Jongstra, M. I. Cybulsky, and J. Jongstra-Bilen. 2002. Modulation of Mac-1 (CD11b/CD18)-mediated adhesion by the leukocyte-specific protein 1 is key to its role in neutrophil polarization and chemotaxis. *J. Immunol.* 169: 415–423.
35. Touret, N., P. Paroutis, M. Terebiznik, R. E. Harrison, S. Trombetta, M. Pypaert, A. Chow, A. Jiang, J. Shaw, C. Yip, et al. 2005. Quantitative and dynamic assessment of the contribution of the ER to phagosome formation. *Cell* 123: 157–170.
36. Laemmli, U. K. 1970. Cleavage of structural proteins during the assembly of the head of bacteriophage T4. *Nature* 227: 680–685.
37. Weil, D., M. A. Power, S. I. Smith, and C. L. Li. 1997. Predominant expression of murine Bmx tyrosine kinase in the granulo-monocytic lineage. *Blood* 90: 4332–4340.
38. Mahajan, S., S. Ghosh, E. A. Sudbeck, Y. Zheng, S. Downs, M. Hupke, and F. M. Uckun. 1999. Rational design and synthesis of a novel anti-leukemic agent targeting Bruton's tyrosine kinase (BTK), LFM-A13 [α-cyano-β-hydroxy-β methyl-*N*-(2,5-dibromophenyl) propenamide]. *J. Biol. Chem.* 274: 9587–9599.
39. Uckun, F. M., A. Vassilev, S. Bartell, Y. Zheng, S. Mahajan, and H. E. Tibbles. 2003. The anti-leukemic Bruton's tyrosine kinase inhibitor α-cyano-β-hydroxy-β-methyl-*N*-(2,5-dibromophenyl) propenamide (LFM-A13) prevents fatal thromboembolism. *Leuk. Lymphoma* 44: 1569–1577.
40. van den Akker, E., T. B. van Dijk, U. Schmidt, L. Felida, H. Beug, B. Löwenberg, and M. von Lindern. 2004. The Btk inhibitor LFM-A13 is a potent inhibitor of Jak2 kinase activity. *Biol. Chem.* 385: 409–413.
41. Varnai, P., K. I. Rother, and T. Balla. 1999. Phosphatidylinositol 3-kinase-dependent membrane association of the Bruton's tyrosine kinase pleckstrin homology domain visualized in single living cells. *J. Biol. Chem.* 274: 10983–10989.
42. Marshall, J. G., J. W. Booth, V. Stambolic, T. Mak, T. Balla, A. D. Schreiber, T. Meyer, and S. Grinstein. 2001. Restricted accumulation of phosphatidylinositol 3-kinase products in a plasmalemmal subdomain during Fcγ receptor-mediated phagocytosis. *J. Cell Biol.* 153: 1369–1380.
43. Kawakami, Y., J. Kitaura, D. Hata, L. Yao, and T. Kawakami. 1999. Functions of Bruton's tyrosine kinase in mast and B cells. *J. Leukocyte Biol.* 65: 286–290.
44. Hempel, W. M., R. C. Schatzman, and A. L. DeFranco. 1992. Tyrosine phosphorylation of phospholipase C-γ2 upon cross-linking of membrane Ig on murine B lymphocytes. *J. Immunol.* 148: 3021–3027.
45. Yokozeki, T., K. Adler, D. Lankar, and C. Bonnerot. 2003. B cell receptor-mediated Syk-independent activation of phosphatidylinositol 3-kinase, Ras, and mitogen-activated protein kinase pathways. *J. Immunol.* 171: 1328–1335.
46. Oancea, E., M. N. Teruel, A. F. Quest, and T. Meyer. 1998. Green fluorescent protein (GFP)-tagged cysteine-rich domains from protein kinase C as fluorescent indicators for diacylglycerol signaling in living cells. *J. Cell Biol.* 140: 485–498.
47. Mukhopadhyay, S., M. Mohanty, A. Mangla, A. George, V. Bal, S. Rath, and B. Ravindran. 2002. Macrophage effector functions controlled by Bruton's tyrosine kinase are more crucial than the cytokine balance of T cell responses for microfilarial clearance. *J. Immunol.* 168: 2914–2921.
48. Saito, K., A. M. Scharenberg, and J. P. Kinet. 2001. Interaction between the Btk PH domain and phosphatidylinositol-3,4,5-trisphosphate directly regulates Btk. *J. Biol. Chem.* 276: 16201–16206.
49. Huang, Y., and J. K. Burkhardt. 2007. T-cell-receptor-dependent actin regulatory mechanisms. *J. Cell. Sci.* 120: 723–730.
50. Labno, C. M., C. M. Lewis, D. You, D. W. Leung, A. Takesono, N. Kamberos, A. Seth, L. D. Finkelstein, M. K. Rosen, P. L. Schwartzberg, and J. K. Burkhardt. 2003. Itk functions to control actin polymerization at the immune synapse through localized activation of Cdc42 and WASP. *Curr. Biol.* 13: 1619–1624.
51. Tomlinson, M. G., L. P. Kane, J. Su, T. A. Kadlecek, M. N. Mollenauer, and A. Weiss. 2004. Expression and function of Tec, Itk, and Btk in lymphocytes: evidence for a unique role for Tec. *Mol. Cell. Biol.* 24: 2455–2466.
52. Scott, C. C., W. Dobson, R. J. Botelho, N. Coady-Osberg, P. Chavrier, D. A. Knecht, C. Heath, P. Stahl, and S. Grinstein. 2005. Phosphatidylinositol-4,5-bisphosphate hydrolysis directs actin remodeling during phagocytosis. *J. Cell Biol.* 169: 139–149.
53. Baba, Y., S. Nonoyama, M. Matsushita, T. Yamadori, S. Hashimoto, K. Imai, S. Arai, T. Kunikata, M. Kurimoto, T. Kurosaki, et al. 1999. Involvement of Wiskott-Aldrich syndrome protein in B-cell cytoplasmic tyrosine kinase pathway. *Blood* 93: 2003–2012.
54. Bunnell, S. C., P. A. Henry, R. Kolluri, T. Kirchhausen, R. J. Rickles, and L. J. Berg. 1996. Identification of Itk/Tsk Src homology 3 domain ligands. *J. Biol. Chem.* 271: 25646–25656.
55. Su, Y. W., Y. Zhang, J. Schweikert, G. A. Koretzky, M. Reth, and J. Wienands. 1999. Interaction of SLP adaptors with the SH2 domain of Tec family kinases. *Eur. J. Immunol.* 29: 3702–3711.
56. Coppolino, M. G., M. Krause, P. Hagendorff, D. A. Monner, W. Trimble, S. Grinstein, J. Wehland, and A. S. Sechi. 2001. Evidence for a molecular complex consisting of Fyb/SLAP, SLP-76, Nck, VASP and WASP that links the actin cytoskeleton to Fcγ receptor signalling during phagocytosis. *J. Cell Sci.* 114: 4307–4318.
57. Ellmeier, W., S. Jung, M. J. Sunshine, F. Hatam, Y. Xu, D. Baltimore, H. Mano, and D. R. Littman. 2000. Severe B cell deficiency in mice lacking the tec kinase family members Tec and Btk. *J. Exp. Med.* 192: 1611–1624.
58. Schaeffer, E. M., J. Debnath, G. Yap, D. McVicar, X. C. Liao, D. R. Littman, A. Sher, H. E. Varmus, M. J. Lenardo, and P. L. Schwartzberg. 1999. Requirement for Tec kinases Rlk and Itk in T cell receptor signaling and immunity. *Science* 284: 638–641.
59. Vieira, O. V., R. J. Botelho, and S. Grinstein. 2002. Phagosome maturation: aging gracefully. *Biochem. J.* 366: 689–704.
60. Yeung, T., B. Ozdamar, P. Paroutis, and S. Grinstein. 2006. Lipid metabolism and dynamics during phagocytosis. *Curr. Opin. Cell. Biol.* 18: 429–437.
61. Defacque, H., E. Bos, B. Garvalov, C. Barret, C. Roy, P. Mangeat, H. W. Shin, V. Rybin, and G. Griffiths. 2002. Phosphoinositides regulate membrane-dependent actin assembly by latex bead phagosomes. *Mol. Biol. Cell* 13: 1190–1202.
62. Ebinu, J. O., D. A. Bottorff, E. Y. Chan, S. L. Stang, R. J. Dunn, and J. C. Stone. 1998. RasGRP, a Ras guanyl nucleotide-releasing protein with calcium- and diacylglycerol-binding motifs. *Science* 280: 1082–1086.
63. Ebinu, J. O., S. L. Stang, C. Teixeira, D. A. Bottorff, J. Hooton, P. M. Blumberg, M. Barry, R. C. Bleakley, H. L. Ostergaard, and J. C. Stone. 2000. RasGRP links T-cell receptor signaling to Ras. *Blood* 95: 3199–3203.
64. Carrasco, S., and I. Mérida. 2007. Diacylglycerol, when simplicity becomes complex. *Trends Biochem. Sci.* 32: 27–36.
65. Topham, M. K. 2006. Signaling roles of diacylglycerol kinases. *J. Cell. Biochem.* 97: 474–484.